Neutrino Oscillation Experiments

Leslie Camilleri
CERN, 1211 Geneva 23, Switzerland

Abstract

Neutrino oscillation experiments ($\nu_\mu \rightarrow \nu_e$ and $\nu_\mu \rightarrow \nu_\tau$) currently being performed at accelerators are reviewed. Future plans for short and long base-line experiments are summarized.

1 Introduction

Under the assumption that neutrinos are massive and that mixing in the lepton sector can be described by a unitary matrix U_{fk} similar to the Cabibbo-Kobayashi Maskawa matrix [1] in the quark sector, then the weak eigenstates ν_e, ν_μ, ν_τ are related to the mass eigenstates ν_1, ν_2, ν_3 by the transformation:

$$|\nu_f >= \sum_{k=1}^{3} U_{fk} |\nu_k > \qquad k = 1,2,3 \qquad f = e, \mu, \tau$$

This allows oscillations [2] to occur. In the case of two-neutrino mixing, such as ν_μ and ν_τ, the probability for finding a ν_τ having started with a ν_μ is given by $P_{\mu\rightarrow\tau} = \sin^2 2\theta \sin^2 2\pi L/\lambda$ where θ = mixing angle which characterizes the strength of the oscillation, L (km) = distance between source and detector, λ = oscillation length = $5E_\nu(\mathrm{GeV})/\Delta m^2(\mathrm{eV}^2)$ with E_ν = neutrino energy, $\Delta m^2 = m^2_{\nu_1} - m^2_{\nu_2}$.

For the probability of oscillation to be significantly different from zero the smallness of Δm^2 must be compensated by a large L or a small E_ν. For small λ (small E_ν or large Δm^2) several oscillations can occur within the detector and $\sin^2(2\pi L/\lambda)$ averages to $\frac{1}{2}$ yielding

$$P_{\mu\rightarrow\tau} = \frac{1}{2} \sin^2 2\theta.$$

The present state of the exclusion plot for $\nu_\mu \rightarrow \nu_\tau$ is shown in Fig. 1. The best limit at high $\Delta m^2, \sin^2 2\theta < 5 \times 10^{-3}$ at 90% CFL, is set by E531 [3] at Fermilab. Similar limits are set by CHARM II [4] and CCFR [5].

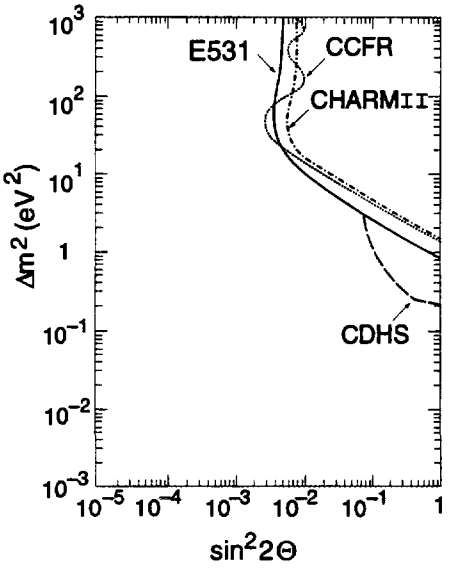

Figure 1: Present state of the $\nu_\mu \rightarrow \nu_\tau$ exclusion plot

2 Observations that Could Benefit from Massive Neutrinos

2.1 Dark matter

If the flat rotational curve of galaxies [6] is interpreted as pointing to the existence of Dark Matter and if this dark matter is identified with the fossil neutrinos left over from the Big Bang, from the density of those neutrinos, 100 $(\nu + \overline{\nu})$ of each flavour per cm^3 and the dark matter density needed to explain the velocity curves, one can infer a neutrino mass of 10 eV/c^2.

2.2 Solar neutrinos

Several experiments [7] have measured the flux of solar neutrinos on earth and found a deficit. The results of the four experiments, combined with the measured luminosity of the sun, indicate that all the pp neutrinos 43% of the boron neutrinos and none of the beryllium neutrinos are observed. This is difficult to understand in terms of a deficiency of the solar models [8] since the beryllium and the boron neutrinos have the same "origin". One possible explanation is that ν_e neutrinos produced in the sun oscillate, on the way to earth, to other types of neutrinos, to which the experiments are not as sensitive. In particular Mikheyev, Smirnov and Wolfenstein (MSW) have proposed a model [9], in which the mixing angle in matter θ_m is related to the mixing angle in vacuum θ_v, the density of the sun, ρ_{SUN}, and the neutrino energy E_ν by:

$$\tan 2\theta_m = \frac{\sin 2\theta_v}{\cos 2\theta_v - \frac{0.76\times10^{-7}\rho_{Sun}E_\nu}{\Delta m^2}}$$

Maximal mixing happens when the denominator goes to zero. If this happens at the energy of the beryllium neutrinos then a value of Δm^2 of 10^{-5} eV^2 is obtained. If the oscillation is attributed to $\nu_e \rightarrow \nu_\mu$ and assuming that $m_{\nu e} \sim 0$, one can then estimate the mass of the ν_τ through the see-saw mechanism [10] that relates the neutrino masses to the quark masses

$$m_{\nu_e} : m_{\nu_\mu} : m_{\nu_\tau} = m_u^2 : m_c^2 : m_t^2$$

yielding $m_{\nu_\tau} \sim 33$ eV^2.

2.3 Atmospheric neutrinos

Atmospheric neutrinos produced in the decays of pions and kaons themselves produced in the interaction of cosmic rays in the upper atmosphere, have been observed [11] in the Kamiokande experiment and others. The expected ratio of ν_μ's to ν_e's is observed to be close to 1 whereas a ratio of 2 is expected. This also could point to oscillations. A measurement of this ratio as a function of zenith angle for higher energy neutrinos has also been performed by Kamiokande [12]. It indicates that the ν_μ/ν_e ratio is most different from expectations for neutrinos entering the detector from below, that is for neutrinos produced 12 000 km away. If this disagreement with expectations is attributed to $\nu_\mu \rightarrow \nu_\tau$ oscillations then $\Delta m^2 = 1.6 \times 10^{-2}$ eV^2 and $\sin^2 2\theta = 1.0$. To probe this region of Δm^2 would require long baseline experiments.

3 The Experiments

The experiments running or approved to run are listed in Table 1.

Table 1:

Experiment	Accel.	Beam	Typical energy	Distance	Mode	Status start-up
KARMEN	ISIS (Rutherford)	ν_μ $\overline{\nu}_\mu$	0.1 GeV	17 m	$\nu_e, \overline{\nu}_e$ Appear	Running 1990
LSND	LAMPF (Los Alamos)	ν_μ $\overline{\nu}_\mu$	0.1 GeV	27 m	$\nu_e, \overline{\nu}_e$ Appear	Running 1993
CHORUS	SPS (CERN)	ν_μ	30 GeV	800 m	ν_τ Appear	Running 1994
NOMAD	SPS (CERN)	ν_μ	30 GeV	800 m	$\nu\tau$ Appear	Running 1995
E803	MAIN INJ. (Fermilab)	ν_μ	10 GeV	470 m	ν_τ Appear	Approved 2000
ICARUS	CERN → GRAN SASSO	ν_μ	10 GeV	732 km	ν_μ Disap. ν_e Appear.	
MINOS	FERMILAB → SOUDAN	ν_μ	10 GeV	732 km	ν_μ Disap. ν_e Appear.	2000
SUPER KAMIOKANDE	KEK 12 GeV (50 GeV) → Super K	ν_μ	1 GeV	250 km	ν_μ Disap. ν_e Appear.	1998 (2003)

3.1 The KARMEN [13] and LSND [14] experiments

The principle of these two experiments is the same. An 800 MeV proton beam is incident on a target in which the pions produced come to rest. The π^+ (at rest) $\rightarrow$ μ^+ (at rest) $\rightarrow$ e^+ decay chain produces ν_μ's, $\overline{\nu}_\mu$'s and ν_e's. The experiments look for the oscillation of $\overline{\nu}_\mu$'s into $\overline{\nu}_e$'s. These are then observed through the $\overline{\nu}_e p \rightarrow e^+ n$ reaction in which the positron is in the $37 < E_e < 50$ MeV range. The $\overline{\nu}_e$'s in the $\pi^- \rightarrow \mu^- \nu_\mu, \mu^- \rightarrow e^- \nu_\mu \overline{\nu}_e$ chain are suppressed by the π^+/π^- ratio of ~ 8, most (95%) of the π^-'s coming to rest in the beam-stop undergoing capture before decaying, the μ^-'s produced by the 5% of the π^-'s that do decay before capture being themselves mostly (88%) captured from atomic orbits before decay. Altogether the relative yield of these is 7.5×10^{-4}. The two experiments do not use a magnetic field and therefore cannot measure the charge of the observed e^-/e^+.

The KARMEN detector consists of a 56 ton segmented liquid scintillator calorimeter. The energy is measured by pulse height and the position by the cell size. The neutron is identified through photons (8 MeV) it emits in its interaction with gadolinium located on foils placed between the calorimeter cells. The neutron travels typically 1 m before interacting and the photons are emitted within 250 μs of the positron detection time. The detector is located 17 m from the target and at 90° to the incident beam direction. The time structure of the KARMEN machine, two 100 ns pulses separated by 330 ns, and a repetition rate of 50 Hz, results in the $\overline{\nu}_e$'s being expected mostly at a time of no accelerator activity, the muon lifetime being 2.3 μs.

The candidate events for $\overline{\nu}_e$'s do not exhibit a time distribution relative to the beam on target time characteristic of the muon lifetime thus leading KARMEN to conclude that no $\overline{\nu}_\mu \rightarrow \overline{\nu}_e$ oscillations are observed at the level of $\sin^2 2\theta < 7.5 \times 10^{-3}$ at large Δm^2. The experiment also sets a limit of $\sin^2 2\theta < 3.8 \times 10^{-2}$ for $\nu_\mu \rightarrow \nu_e$ oscillations through the non observation of $\nu_e C \rightarrow e^- N$ in the E_{e^-} range 60 $\rightarrow$ 180 MeV. KARMEN is currently being upgraded with a better veto shield which will allow its sensitivity to be improved by a factor of 10 within a few years.

The LSND detector consists of a 180 ton tank of liquid scintillator. The energy is measured both through the pulse height of the scintillator light and the radius of the Čerenkov ring emitted by the electron, both being detected by photomultipliers lining the inner surface of the tank. The position of the particles is determined using phototube timing. The neutron is identified as in KARMEN except that the photons are emitted through its interaction with the protons in the scintillator: $np \rightarrow d\gamma(E_\gamma = 2.2$ MeV). The detector is located 27 m from the target at an angle of 17° to the beam. The time structure of the LAMPF accelerator, a 500 μs continuous spill repeated every 8.3 ms makes the detection of the expected $\overline{\nu}_e$'s coincident with accelerator activity, unlike KARMEN. Because of this long spill the requirement that the events be observed with the characteristic muon lifetime distribution relative to beam on target time, cannot be used by LSND. They discriminate between background events and signal events using a likelihood: R, computed for each event and based on the difference in position between the positron and the photon, the difference in time between the positron and the photon and the photon pulse height. The positron energy distribution for events with $R > 30$ is shown in fig. 2 together with the expected background.

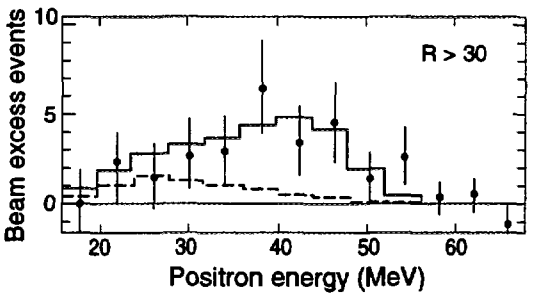

Figure 2: The positron energy distribution obtained by LSND for the likelihood R (defined in the text) greater than 30.

A total of 22 events are seen in the interval $36 < E_e < 60$ MeV, where 2.5 background events are expected from non-beam sources and 2.14±0.4 from beam-related sources. A fit of the overall likelihood distribution for events with $20 < E_e < 60$ MeV, to a sum of correlated and uncorrelated neutron-positron distributions yields a total of $51.8^{+18.7}_{-16.9}$ candidate events and an oscillation probability of $(0.31^{+0.11}_{-0.10} \pm 0.05)\%$. The expected energy distribution including an oscillation contribution with large Δm^2 is also shown in fig. 2. The regions of 90% and 99% CFL obtained by LSND are shown in fig. 3 together with the limits set by KARMEN, E776 [15] and the Bugey [16]. There is a region at $\Delta m^2 < 2 - 3eV^2$ that could still satisfy all the experiments.

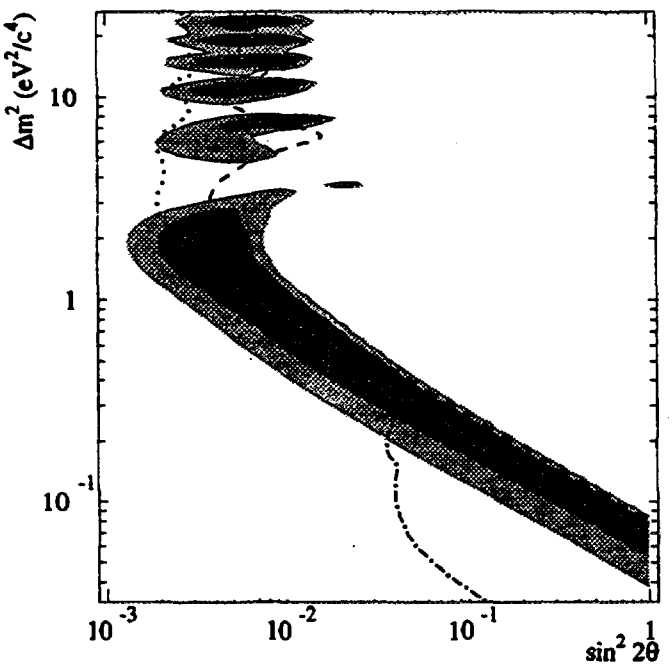

Figure 3: The LSND Δm^2 vs $\sin^2 2\theta$ favoured regions. The darkly shaded and lightly shaded regions are the 90% and 99% likelihood regions. Dashed curve: KARMEN, Dotted curve: E776, dot-dashed curve: Bugey.

3.2 The neutrino oscillation experiments at CERN

There are two experiments, the CERN Hybrid Oscillation Research Apparatus (CHORUS) [17] and the Neutrino Oscillation Magnetic Detector (NOMAD) [18]. Both are looking for $\nu_\mu \rightarrow \nu_\tau$ oscillations through the appearance of ν_τ's in a ν_μ beam. The ν_τ is searched for through its charged current interaction $\nu_\tau N \rightarrow \tau^- X$.

The 450 GeV/c protons accelerated by the SPS are directed onto a target to produce pions and kaons which subsequently decay giving neutrinos. The target is made of beryllium, a low atomic number material, to reduce multiple scattering and avoid widening of the beam. The target has a small diameter (3 mm) to avoid reinteraction of secondaries and therefore degradation of the energy spectrum, and is long enough (1.1 m) to allow 93% of the protons to interact. The secondaries of a given sign are focused into a parallel beam by two magnetic horns. These horns consisting of two coaxial current sheets providing a toroidal field run at currents of 100 kA. They must therefore be pulsed. For this reason and in order to reduce cosmic ray background, the protons are delivered to the target in two 6 ms long spills at each SPS cycle. The horns are followed by a 290 m long evacuated decay tunnel. The muons are bent away by a magnetic iron toroid and ranged out by shielding. About 2.5×10^{13} protons are incident on the beryllium target every 14.4 s. The beam composition is $\nu_\mu : \overline{\nu}_\mu : \nu_e : \overline{\nu}_e = 1 : 0.054 : 0.009 : 0.002$.

The intrinsic fraction of ν_τ's in the beam, coming from the decay of D_S mesons produced in the target is estimated [19] to be $\sim 5 \times 10^{-6}$ which is negligibly small. CHORUS started running in 1994 and has collected 3.1×10^{19} protons on target (pots) whereas NOMAD started in 1995 and has collected 1.8×10^{19} pots. Both experiments will run until the end of 1997.

NOMAD (fig. 4) intends to distinguish $\nu_\tau N \rightarrow \tau^- X$ events from background using kinematical cuts such as missing P_T, angular correlations etc. To do so very good energy, momentum and angular resolutions are needed. The τ is detected through its $e\,\overline{\nu}_e\nu_\tau$, $\mu\overline{\nu}_\mu\nu_\tau$, $\pi^-\nu_\tau$, $\rho^-\nu_\tau$, $\pi^+\pi^-\pi^-(n\pi^0)\nu_\tau$ decay modes for a total of 83% of its branching ratio. The target consists of the walls of the drift chambers used for momentum measurement: 132 planes spread over 4 m amounting to 3 tons in mass and to only 1 radiation length in total. The experiment reuses the UA1 magnet inside which the drift chambers are placed. The momentum resolution, $\sigma(p)/p$, for an average length track varies between 3 and 5% over the momentum range relevant to the measurement. The electromagnetic calorimeter needed to identify electrons and measure photons consists of lead glass and has an energy resolution of $\sigma(E)/E = 0.04/\sqrt{E} + 0.01$.

The discrimination between electrons and pions is provided by 9 transition radiation modules each consisting of 350 foils of polypropylene followed by a plane of 176 straw tubes containing a xenon-methane mixture to detect the transition radiation X-rays. A preshower consisting of a lead sheet followed by two planes of proportional tubes provides further e/π separation. Chambers behind walls of iron provide muon identification. Some of this iron has been instrumented to provide a hadron calorimeter.

As an example of the type of cuts used in the analysis, the electronic decay of the τ will be considered.

$$\nu_\tau N \rightarrow X\tau^- \rightarrow e^-\overline{\nu}_e\nu_\tau$$

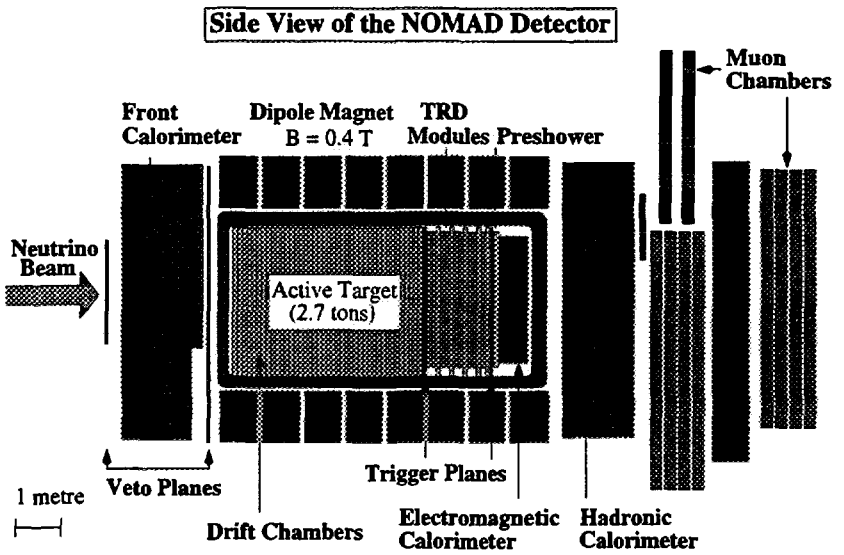

Figure 4: The NOMAD detector

The major background to this channel is caused by charged current interactions of the $\sim 1\%$ ν_e component of the beam $\nu_e N \rightarrow Xe^-$.

In the plane perpendicular to the beam direction, angles between the electron and the resultant hadron vector, ϕ_{eh}, and between the missing P_T and the resultant hadron vector, ϕ_{mh}, are defined (fig. 5a,b). For the background reaction, since the electron and the hadrons are the only particles in the reaction, the Monte Carlo distribution for ϕ_{eh} is sharply peaked at π (fig. 5c). For the τ reaction, the τ is back to back to the hadrons, but the electron from its decay will not be necessarily back to back with the hadron (fig. 5d). In the background reaction any missing P_T will arise either from missed particles or from mismeasurements resulting in a flat ϕ_{mh} distribution (fig. 5e). In the τ reaction the missing P_T will be due to the two missing neutrinos and will be centered on the τ direction, resulting in a peak in ϕ_{mh} at π (fig. 5f). The ϕ_{eh} and ϕ_{mh} distributions are quite different for the background and signal.

The number of events expected to be seen by NOMAD for an exposure of 2.4×10^{19} pots, should oscillations occur just at the present limit of $\sin^2 2\theta = 5 \times 10^{-3}$ is listed in Table 2, together with the number of background events expected in each of the τ decay modes. With these numbers NOMAD will be able to set a limit of $\sin^2 2\theta < 3.8 \times 10^{-4}$ at 90% CFL for high Δm^2. Note that should any significant number of candidates be observed, they will have to be distributed among the various decay channels according to the various branching ratios and efficiencies.

NOMAD has very good electron identification and can therefore make a thorough study of ν_e CC events coming from the small (1%) ν_e content of the beam. By studying the $E_{vis}(= E_e + E_{hadrons} = E_\nu)$ distribution of these ν_e CC events and comparing it to the one expected, an additional contribution due to $\nu_\mu \rightarrow \nu_e$ oscillations can be looked for. The difficulty of this measurement is that it requires a very good knowledge of the "standard" ν_e component of the beam. It is expected that significant oscillations limits could be set at the high Δm^2 end of the LSND favoured region.

The principle used by CHORUS (fig. 6a) to recognise the presence of a τ meson is to observe the finite path of the τ meson before it decays. Because τ decay paths are < 1 mm at these energies the target must be active and have very good spatial resolution. This has led to the use of emulsions. A total of 800 kg will be used amounting to 4 radiation lengths. A detail of the target area is shown in Fig. 6b.

Table 2:

Channel	Expected number of events $\sin^2 2\theta = 5 \times 10^{-3}$ and large Δm^2	Background events
$\tau \rightarrow e\nu\nu$	39	4.6
$\mu\nu\nu$	11	2.0
$\pi\nu$	3	< 0.2
$\rho\nu$	7	< 0.2
$3\pi\nu + (\geq 0\pi^0)$	18	< 0.2
Total	78	7

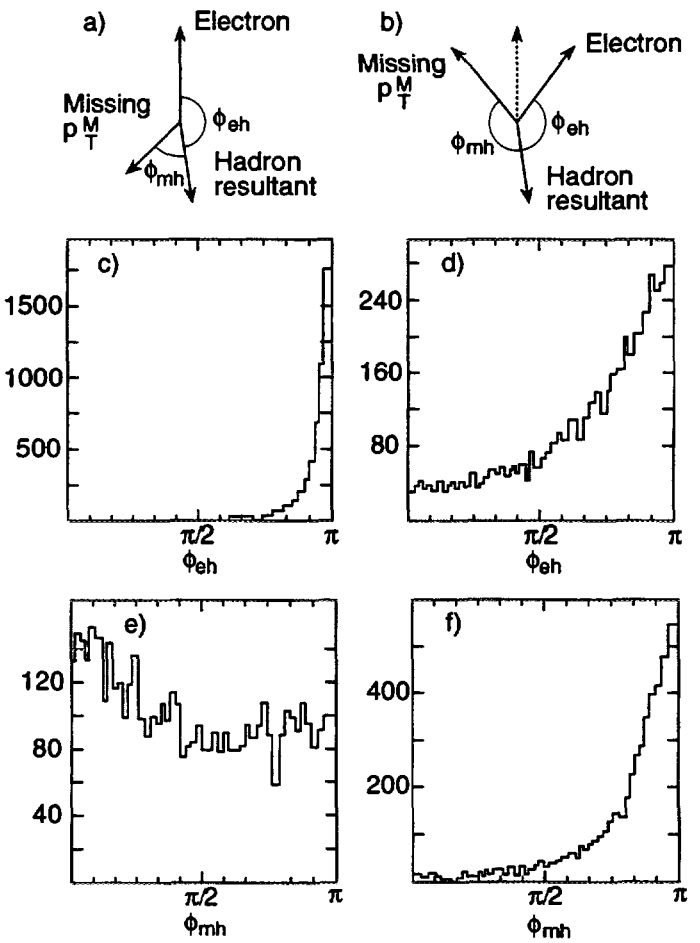

Figure 5: Definition of ϕ_{eh} and ϕ_{mh} and representative Monte Carlo distributions of these variables for ν_e CC and $\nu_\tau(\tau \rightarrow e)$ events

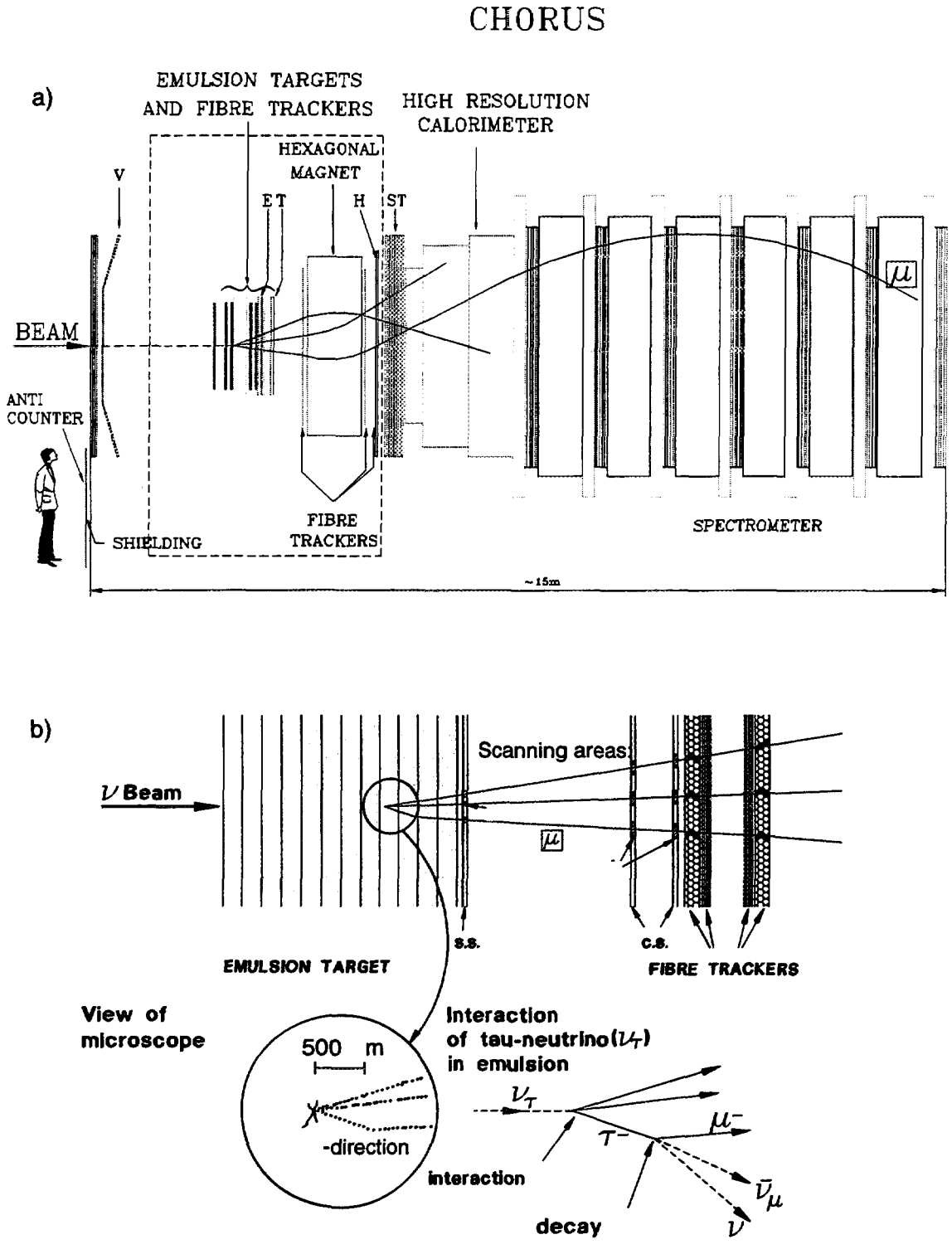

Figure 6: a) The CHORUS detector b) A detail of the CHORUS emulsions

A bulk emulsion stack which remains in place for two years is followed by sheets which are changed more often and will therefore have less occupancy and by scintillation fiber trackers. An hexagonal magnet giving a toroidal field provides a momentum resolution of 16% at 2 GeV/c rising to 23% at 10 GeV/c. The spectrometer is followed by an electromagnetic calorimeter and by a muon detector.

The number of events to be scanned is reduced by a factor of 10 by applying loose kinematics cuts of the type used by NOMAD. In the surviving events, tracks reconstructed in the spectrometer are extrapolated to the emulsions in order to determine where to scan. These tracks are followed into the emulsions to look for a kink with a P_T relative to the candidate τ direction of at least 0.24 GeV/c. The magnitude of this kink P_T is determined using the momentum of the track as determined by the spectrometer and the angle of the kink as determined by the tracking in the emulsion. A charm decay observed in the CHORUS emulsion is shown in fig. 7.

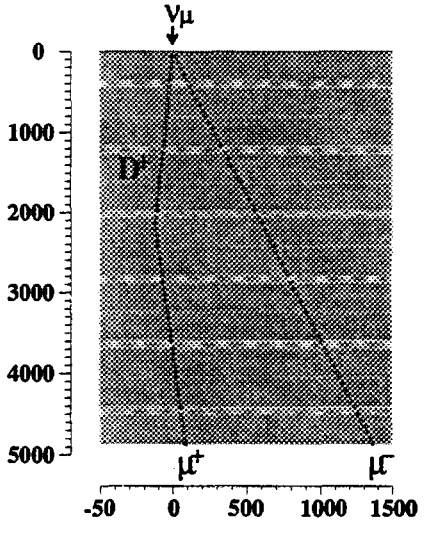

Figure 7: A charm decay observed in CHORUS

The major background to the muonic channel comes from the semileptonic decays of negative charmed particles produced by the $\overline{\nu}_\mu$ and $\overline{\nu}_e$ components of the beam coupled with missing the accompanying μ^+ or e^+. The finite travel of the D^- before its decay can thus simulate a τ decay.

In the $\tau^- \rightarrow \pi^- \nu_\tau$ channel, the major background is due to hadrons from a neutral current interaction scattering close to the vertex without any visible recoil activity. These "white star" kinks are very much reduced by requiring the P_T of the kink to be at least 0.24 GeV/c. Further background reduction can be obtained by comparing the direction of the hadronic momentum vector as calculated using the spectrometer with the direction of the τ candidate track as measured in the emulsions. For genuine τ decays these two vectors must be back to back in the plane transverse to the beam. Although the neutrinos from the τ decays are not observed, enough kinematic variables are measured to be able to estimate the ν_τ energy for each candidate event. If enough candidates are recorded the shape of the $E_{\nu\tau}$ distribution will provide a measure of Δm^2. If oscillations occur at the E531 limit 64 events

are expected with 0.4 background events. The expected sensitivity of CHORUS after a four year run will be $\sin^2 2\theta < 2 \times 10^{-4}$ at 90% CFL for high Δm^2.

3.3 E803 (COSMOS)

This experiment [20] will run at Fermilab with the new main injector. The detector, fig. 8, is very similar to CHORUS. Emulsion stacks comprising both fixed bulk emulsions and changeable sheets are followed by fibre trackers, a magnet, drift chambers, an electromagnetic calorimeter and a muon detector. However the high repetition rate of the main injector should allow E803 to collect 1.3×10^{21} protons on target as opposed to 4.5×10^{19} for CHORUS. The background in E803 is similar to that described for CHORUS. However, the better momentum resolution of E803 (3%) should allow a better rejection of the background: for the $\tau^- \rightarrow \pi^- \nu_\tau$ mode, a plot of the kink P_T relative to the τ direction should display the characteristic Jacobian peak at $\sim m_\tau/2$ (fig. 9). A limit of 2.8×10^{-5} in $\sin^2 2\theta$ is expected to be set by E803.

The expected exclusion plot for the three $\nu_\mu \rightarrow \nu_\tau$ oscillation experiments is shown in Fig. 10. Over the next 10 years the E531 limit on $\sin^2 2\theta$ at large Δm^2 should be improved by more than two orders of magnitude and at large mixing, the Δm^2 limit will be improved by about a factor of 5 down to the 1 eV^2 range.

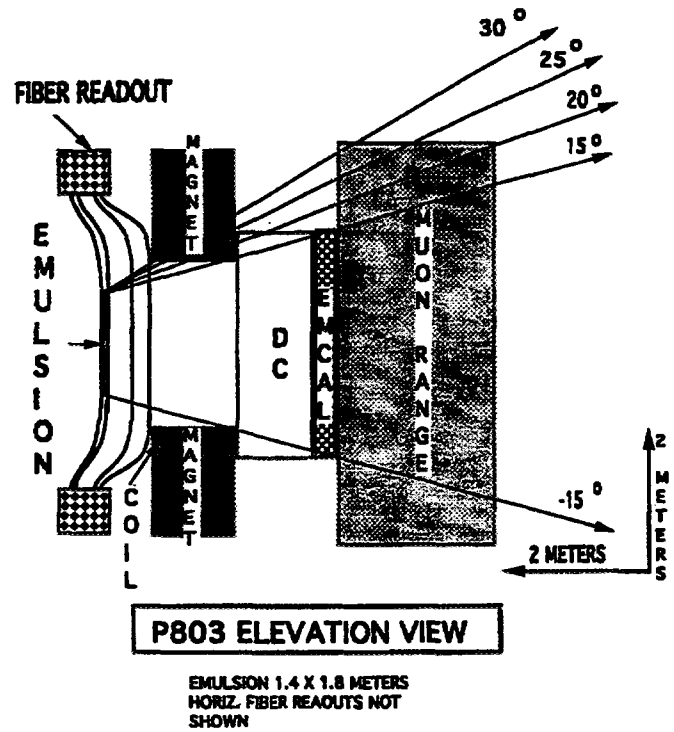

Figure 8: The E803 detector

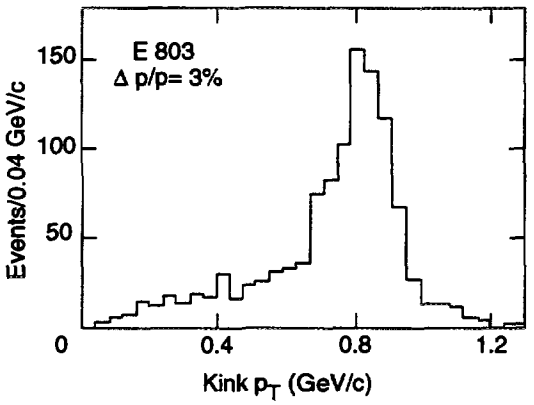

Figure 9: The Jacobian peak in the P_{TKINK} distribution expected from $\tau \rightarrow \pi\nu$ decays

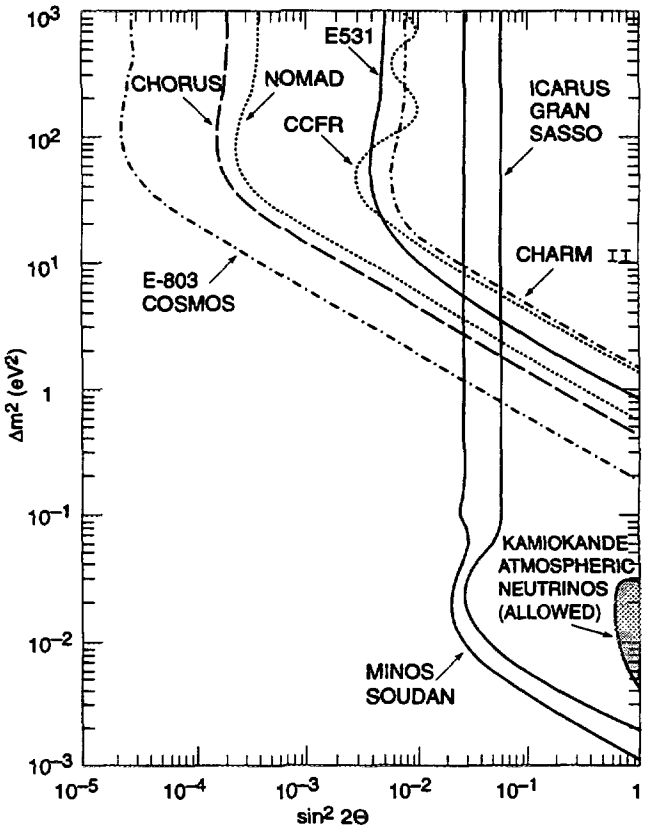

Figure 10: The regions of the $\Delta m^2 - \sin^2 2\theta$ plot expected to be excluded by NOMAD, CHORUS, E803, ICARUS and MINOS

3.4 Future ideas at CERN

Meetings between CHORUS, NOMAD and other interested physicists, including the proponents of an Argon TPC neutrino experiment ALADINO [21] and of a water Čerenkov counter experiment [22] are currently taking place. One possibility would be to combine the good kinematical discrimination of NOMAD with the good spatial resolution of CHORUS.

Such a detector could consist of an active target weighing 900 kg and consisting of planes of silicon (40 m^2 in total) interleaved with passive material such as boron carbide [23]. The active target would be followed by a spectrometer such as the one used by NOMAD. The silicon planes would provide a measurement of the impact parameter at the primary vertex for candidate pions from $\tau \rightarrow \pi^- \nu_\tau$ decays or displaced vertex identification for $\tau \rightarrow 3\pi\nu_\tau$ candidate decays. These additional constraints would allow much looser kinematic cuts to be applied thus greatly improving the τ detection efficiency and hence the sensitivity of the experiment. A four-year run could reach a sensitivity of $\sin^2 2\theta < 1.9 \times 10^{-5}$ at 90% CFL.

A prototype of such a detector [24] is currently being built and will be installed in NOMAD in time for the 1997 run. It should provide enough neutrino interactions to allow the measurement of the resolution function for the impact parameter and displaced vertex under realistic conditions. Two variants on this scheme are also being studied.

- Replacing the silicon by 20 μm capillaries filled with liquid scintillator and read by image intensifiers. This technique is currently being studied in CHORUS.

- Replacing the boron carbide with emulsion sheets [25]. Here the silicon impact parameter capabilities would only be used for a fast selection of events of interest which would then be scanned. This reduction of the number of events to be scanned would allow an increase in the total emulsion mass used.

ALADINO [21] is a proposal to install a 400 ton liquid argon TPC in the present neutrino beam line behind CHORUS and NOMAD. The optics of the beam would be changed to provide a lower neutrino energy and a narrower energy distribution. The physics addressed is $\nu_\mu \rightarrow \nu_\tau$ oscillations through the detection of quasi-elastic ν_τ CC interactions with the subsequent electronic decay of the τ. The experiment would also measure $\nu_\mu \rightarrow \nu_e$ oscillations again using quasi-elastic events. The expected snsitivities at high Δm^2 are $\sin^2 2\theta < 6 \times 10^{-5}$ for $\nu_\mu \rightarrow \nu_\tau$ oscillations and $\sin^2 2\theta < 6.4 \times 10^{-4}$ for $\nu_\mu \rightarrow \nu_e$ oscillations.

3.5 Long base-line experiments

This involves sending neutrino beams produced at an accelerator to an underground detector located several hundred kilometres away. Three such projects are currently under way or being considered.

1) Sending a beam from KEK to the Superkamiokande detector located 250 km away [26]. The present accelerator can provide a neutrino beam of mean energy 1 GeV. This will happen in 1998 and the first priority is to look for $\nu_\mu \rightarrow \nu_e$ oscillations and check the atmospheric neutrino results. A 50 GeV synchrotron is currently being planned at KEK. A neutrino beam from this machine and directed at Superkamiokande would allow $\nu_\mu \rightarrow \nu_\tau$ oscillation experiments as well starting in 2003.

2) A beam from the SPS, different from the present neutrino beam, could be directed at detectors located in the Gran Sasso laboratory, 732 km away. Detectors based on a liquid argon TPC (ICARUS)[27] or on an iron filings + scintillator calorimeter (NOE) [28] are being discussed. An ICARUS prototype module weighing 600 tons will be installed in the Gran Sasso laboratory in 1998. The final design would probably involve 10 such modules.

3) It has been decided to direct a Fermilab neutrino beam to a detector located in the

SOUDAN mine, MINOS,[29] again 732 km away. The experiment intends to look for $\nu_\mu \rightarrow \nu_\tau$ oscillations and is best done in conjunction with a near detector. The technique is based on a different ratio of charged current (CC) to all events being measured at the two locations. Assuming the oscillation wavelength is comparable to 700 km, the near detector would then measure the "correct" CC/ALL ratio. However if ν_μ's oscillate to ν_τ's only 17% of the ν_τ's decay to muons and would look like charged current events, whereas 83% would look like neutral currents. Therefore

$$\frac{CC}{ALL}|_{FAR} < \frac{CC}{ALL}|_{NEAR}.$$

When including the future long base-line results, the $\nu_\mu - \nu_\tau$ exclusion plot would then look as shown in fig. 10-. As can be seen a large fraction of the area pointed to by the current "anomalous" results will have been covered. As can also be noted the field is exceedingly active, with experiments running, being built and being proposed on many continents.

References

[1] M.Kobayashi and M.Maskawa, Progr. Theor. Phys. **49** (1973) 652.

[2] B.Pontecarvo, Zh. Eksp. Theor. Fiz. **33** (1957) 549 and **34** (1958) 247.

[3] N.Ushida et al,. Phys. Rev. Lett. **57** (1986) 2897.

[4] M.Gruwé et al., Phys. Lett. **B309** (1993) 463.

[5] K.S.McFarland et al., Phys. Rev. Lett. **75** (1995) 3993.

[6] S.F.Shandarin. Massive Neutrinos and Cosmology in Neutrino Physics edited by Klaus Winter (Cambridge Monographs on Particle Physics, Nuclear Physics and Cosmology) p. 645 and references therein.

[7] HOMESTAKE: R.Davis, Prog. Part. Nucl. Phys. **32** (1994) 13;
KAMIOKANDE: Y.Suzuki et al., Nucl. Phys. B (Proc. Suppl) **38** (1995) 54;
SAGE: J.N.Abdurashitov et al., Phys. Lett. **B328** (1994) 234;
GALLEX: P.Anselmann et al., Nucl. Phys. (Proc. Suppl.) **B38** (1995) 68.

[8] J.N.Bahcall and R.K.Ulrich, Rev. Mod. Phys. **60** (1988) 297 and references therein;
J.N.Bahcall and M.H.Pinsonneault, Rev. Mod. Phys. **64** (1992) 885;
S.Turck-Chieze and I.Lopes, Astrophys. J. **408** (1993) 347.

[9] L.Wolfenstein, Phys. Rev. **D17** (1978),2369;
S.P.Mikheyev and A.Y.Smirnov, Sov. J. Nucl. Phys. **42** (1985) 913.

[10] M.Gell-Mann, P.Ramond and R.Slansky *in* Supergravity, eds. P.van Nieuwenhuizen and D.Freeman (North Holland, Amsterdam, 1979) p. 315;
T.Yanagida, Progr. Theor. Phys. **B135** (1978) 66.

[11] K.S.Hirata et al., Phys. Lett. **B280** (1992) 146;
D.Casper et al., Phys. Rev. Lett. **66** (1991) 2561.

[12] Y.Fukuda et al., Phys. Lett. **B335** (1994) 237.

[13] B.Armbruster et al., Nucl. Phys. (Proc. Suppl.) **38** (1995) 235.

[14] C.Athanassapoulos et al., Phys. Rev. Lett **B75** (1995) 2650.

[15] L.Borodovsky et al., Phys. Rev. Lett. **68** (1992) 274.

[16] B.Achkar et al., Nucl. Phys. **B434** (1995) 503.

[17] CERN Hybrid Oscillation Research Apparatus (CHORUS). A new search for $\nu_\mu \rightarrow \nu_\tau$ oscillation, CERN PPE/93–131 and CERN-SPSLC/90–42 SPSC P254.

[18] Neutrino Oscillation Magnetic Detector (NOMAD). Search for the Oscillation $\nu_\mu \rightarrow \nu_\tau$ CERN-SPSLC/91–121 SPSC P261 (1991) and CERN-SPSLC/93–31 SPSLC M525 (1993).

[19] Prompt ν_τ background in Wide Band ν_μ beams. B.Van de Vyver and P.Zuccheli, CERN-PPE 96–113. Submitted to Nucl. Instrum. Methods;
Prompt ν_τ Fluxes in Present and Future Tau Neutrino Experiments. M-C.Gonzalez-Garcia and J-J.Gomez-Cadenas, CERN-PPE 96–114. Submitted to Phys. Rev. D.

[20] COSMOS - Muon Neutrino to Tau Neutrino Oscillations Experiment at Fermilab (E803).

[21] Letter of Intent for a short-baseline experiment with a Liquid Argon TPC, CERN SPSLC 95–37 SPSLC/I205.

[22] T.Ypsilantis et al., Nucl. Instrum. Methods **A371** (1996) 330.

[23] J-J.Gomez-Cadenas et al., Nucl. Instrum. Methods **A378** (1996) 196.

[24] A prototype of an Instrumented Target for the NOMAD detector, CERN SPSLC/96–2, SPSLC/P261/Add.3.

[25] Study of a new experiment for the search for $\nu_\mu - \nu_\tau$ oscillations. A.Ereditato et al., CERN PPE/96–106.

[26] Long Base Line Neutrino Oscillation Experiment (E362) using KEK-PS and Super-Kamiokande.

[27] ICARUS II. A Second Generation Proton Decay Experiment and Neutrino Observatory at the Gran Sasso Laboratory, Proposal by the ICARUS Collaboration (1993).

[28] M.Ambrosio et al., Nucl. Instrum. Methods **A363** (1995) 604.

[29] MINOS: Main Injector Neutrino Oscillation Search (Fermilab E-875).